

## THERMOECONOMIC ANALYSIS OF A KALINA CYCLE FOR WASTE HEAT RECOVERY

**Felipe Raúl Ponce Arrieta, felipe.ponce@pucminas.br**

**Gustavo Rodrigues da Costa Horta, gustavohorta@live.com**

Pontifical Catholic University of Minas Gerais, Av. Dom José Gaspar, 500 - Belo Horizonte - MG Zip Code: 30535-901, Brazil

**Cláudio Homero Ferreira da Silva, chomero@cemig.com.br**

Cemig GT SA, Av. Barbacena, 1200 - 20º andar - Ala B2 - B. Santo Agostinho, 131 - Belo Horizonte - MG Zip Code: 30.190-130, Brazil

**Abstract.** *Thermoeconomic analysis, based on EES (Engineering Equation Solver) model, of a Kalina cycle for waste heat recovery aims to optimize the exergoeconomic indexes of a modified Kalina Cycle with 2 turbines. The model has as the main objective the optimization to minimize the unit exergetic costs and unit exergoeconomic costs and maximize the electric power generation of the Kalina Cycle using the preheater exhaust gases in a 3500 tc/day cement plant. We carried out parametric studies in order to evaluate the best operating point as function of turbine inlet pressure and temperature and ammonia mass fraction concentration in the working fluid. The model uses the thermo physical properties of the working fluid provided by the function NH<sub>3</sub>-H<sub>2</sub>O of the EES library. We implemented the mass, energy and exergy balances for each equipment and a modification of the exergetic cost structural theory. The model includes cost information curves from National Energy Technology Centre (USA) with values corrected to the end of 2013. In the results, we found that the cycle is able to produce 1.780 MW of electric power with a cost of 215 R\$/MWh. The optimized parameters of the cycle are ammonia mass fraction of 0.80, the first turbine inlet pressure of 140 bar, the second turbine inlet pressure of 27 bar and the superheating temperature of 568.15 K. We concluded that the use of a second turbine increase in 633 kW the electricity production but implies in a second subsystem of distillation and absorption, rising the investment costs. In spite of it, the power generation cost is competitive in the existing Brazilian's electric market.*

**Keywords:** *Kalina Cycle, Thermoeconomic analysis, Cycle Configuration, Waste Heat*

### 1. INTRODUCTION AND LITERATURE REVIEW

The cement is one of the most energy intensive industrial process in the world, requiring great amounts of thermal energy; this energy consumption represents approximately 50% to 60% of the production cost of the cement (Mirolli, 2005). The current Brazilian economic and electric scenario creates an attractive environment for recovery of waste heat of cement production. The use of the Kalina cycle has proven to be promising alternative for this use.

Arrieta and Santos (2014) used the preheater gases and the clínquer cooler gases of a 5000 tc/day cement plant in a KCS34 Kalina Cycle and were able to produce about 1.09 kW/tc with the unit exergetic cost of 6.19 kW/kW. Junior and Others (2015) optimized a modified KCS34 for recovery of the pre-heater gases of a 5000 tc/day cement plant, achieving the production of 2803 kW with the cost of 298.8 R\$/MWh. He and others (2014) evaluated a Kalina cycle using a second expander instead of a relief valve, the results show the increase of the exergetic efficiency were about 9.3% when the pressure of expansion were 3 MPa. Arslan (2010) presented a cycle supplied by sources with temperatures ranging between 80°C and 100°C and results for ammonia fractions ranging 0.7 to 0.9, showing the continuous increase in efficiency as the fraction of ammonia also increases. Lolos and Rogdakis (2009) showed that the maximum efficiency of the cycle is maximum when using 95% of ammonia mass fraction in the working fluid. Arrieta and Horta (2014) obtained in their analysis of a simple Kalina cycle the minimum exergetic cost of 1.902 kW/kW when the cycle operates with 473 K. Singh and Kaushik, (2013) demonstrated the optimum ammonia mass fraction in a Kalina cycle increases with the pressure, for the operating pressure of 4 MPa the optimum ammonia mass fraction was 0.8. Rodrigues and others (2013) compared a Kalina Cycle with a Rankine Organic Cycle for geothermal generation in Brazil, the results found show that the Kalina Cycle is more feasible, with the cost of e 0.178 €/kWh, 18% less than the Organic cycle. Elsayed e and others (2013) evaluated the utilization the major binary zeotropic composition for working fluid of Kalina cycle and concluded that the best performance archived was utilizing NH<sub>3</sub>-H<sub>2</sub>O.

The study aimed to calculate the points of greatest thermoeconomic performance, solving the production diagram of the thermal cycle. We aimed also to minimize the exergetic cost for the net power flow and maximize the power output. We analyzed performance graphs of the power output, cost and exergetic cost as a function of ammonia mass fraction and the superheater temperature difference.

The cycle analyzed in this article we present in Figure 1 and is a modification of the Kalina Cycle analyzed by Arrieta and Horta (2013) and work as follow. The working fluid, after partially vaporized in the evaporator, flows to the separator, through the flow 7. It is separated, therefore, into two flows, one rich in ammonia, flow 8, which flows the superheater and weak in ammonia, flow 14, which flows the regenerator 1. The flow 9 after being superheated, is taken

to the turbine 1 by the flow 10 and is expanded, going to the separator 2. Again, the working fluid is separated into two flows, one rich and other poor in ammonia, fluxes 11 and 17 respectively. The flow 11 expands in the turbine 2 and flows to the absorber 2 via flow 12. The weak ammonia flows, 14 and 17, coming from the separator 1 and separator 2 are taken to regenerators 2 and 1 respectively, then these flows 15 and 18 are relieved into the valves 1 and 2 generating flows 16 and 19. The relieved flows are led to the absorber 1 and 2, the absorber 2 the flow 19 is mixed with flow 12 generating flow 13 which is addressed to the regenerator 4, which has as output the flow 23. The flow 20, containing the fraction of heat which cannot be utilized is condensed in the condenser 2, generating the flow 21 which is pressurized in the flow generating 22. Flows 16 and 23 mix in the absorber 1, generating the flow 24, which is goes through the regenerator 3 generating the flow 25. The valve 3 is releases the pressure from the flow 25, generating flow 1, which is condensate generating flow 2 and is pumped by the pump. The flow 3, from the exit of the pump enters the regenerator 3 outputting flow 4 which goes to the regenerator 2, generating the flow 5, going to the regenerator 1, which generates the flow 6 going to the evaporator.

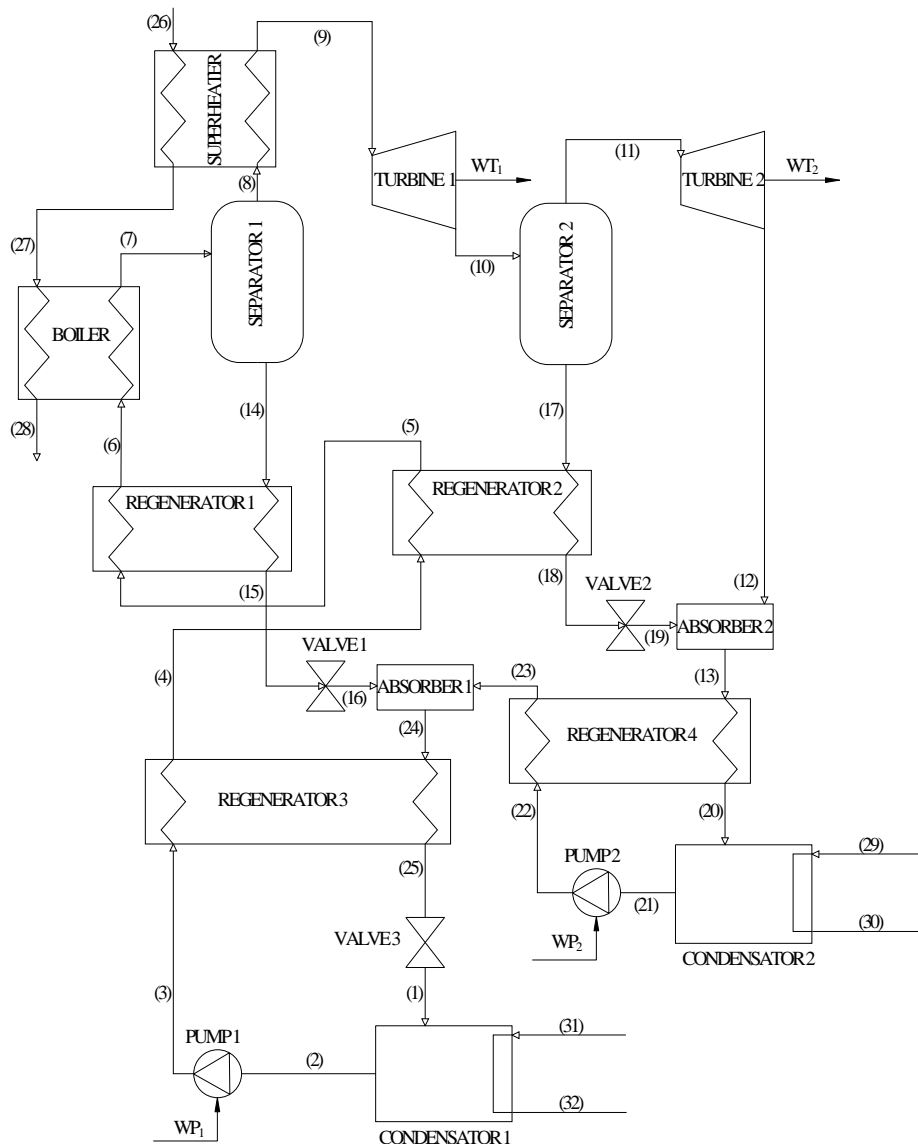


Figure 1. Plant scheme used in the simulation.

## 2. METHODOLOGY

The thermodynamic and thermo-economic modeling and analysis of the present Kalina Cycle has been developed using the algorithm shown in Fig. 2. The model implemented on EES software and used the thermo-physical properties of the working fluid provided by the function  $\text{NH}_3\text{-H}_2\text{O}$  of the EES library. The optimization performed using the genetic algorithm's method provided by EES software. A sensitivity analysis was made of the ammonia mass fraction in the boiler and the difference temperature between the hot exhaust gases and the working fluid.

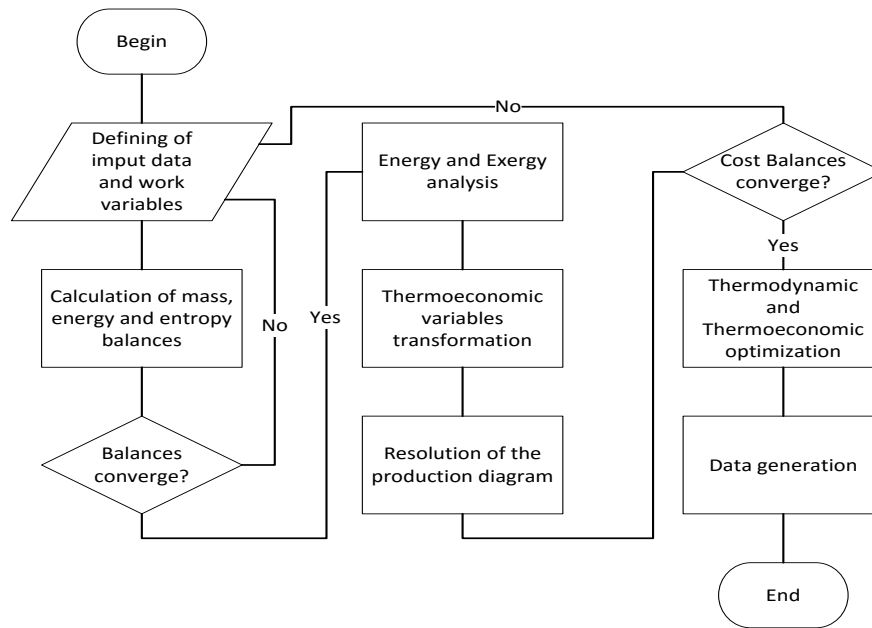


Figure 2. Algorithm model used in the simulation.

We considered the input data from Apodi Cimentos (2016), with a plant's capacity of 3500 tc/d. The preheater exhaust gases used as the primary energy source and its temperature and composition we present in table 1. We defined the minimum outlet temperature of the cycle as 501.15 K.

Table 1. Preheater exhaust gases temperature and composition.

Preheater	
Temperature (K)	583.15
Composition (% of volume)	
N <sub>2</sub>	68.58%
O <sub>2</sub>	4.94%
CO <sub>2</sub>	26.30%
H <sub>2</sub> O	1.18%

The mass, energy and balances for control volume were applied for each equipment and subsystem of the cycle, neglecting the changes in kinetic and potential energy. These balances are given by Eq. (1), Eq. (2) respectively, where  $\dot{m}$  represents the mass flow,  $\dot{Q}$  the heat transfer rate,  $\dot{W}$  the power,  $h$  the specific enthalpy of the mass flow: The subscripts *in* and *out* represent inlet and outlet respectively.

$$\sum \dot{m}_{in} = \sum \dot{m}_{out} \quad (1)$$

$$\dot{Q} - \dot{W} = \sum \dot{m}_{out} \cdot h_{out} - \sum \dot{m}_{in} \cdot h_{in} \quad (2)$$

In exergy analysis, the dead state we defined it at 273.15 K for  $T_0$  and 101.35 kPa for  $P_0$ . We calculated the specific exergy of a flow by Eq. (3) Eq. (4) and Eq. (5). The first equation states that the total specific exergy of a flow,  $ex$ , is given by the sum of its chemical exergy,  $ex_{Ch}$ , and its physical exergy,  $ex_{Ph}$ . The physical exergy evaluation is in Eq. (4).

$$ex = ex_{Ch} + e_{Ph} \quad (3)$$

$$ex_{Ph} = (h - h_0) - T_0 \cdot (s - s_0) \quad (4)$$

We calculated the chemical exergy in function of the quality of the flow. If the quality of the flow is equal or below 0, the chemical exergy is evaluated by Eq. (5), where  $x$  represents the ammonia mass fraction in the flow,  $ex_{Ch,NH_3}^0$  represents the standard chemical exergia of ammonia,  $ex_{Ch,H_2O_L}^0$  represents the standard chemical exergy of liquid water.

$$ex_{Ch} = x \cdot ex_{Ch,NH_3}^0 + (1-x) \cdot ex_{Ch,H_2O_L}^0 \quad (5)$$

If the quality is between 0 and 1, the chemical exergy is calculated using Eq. (6), Eq. (7) and Eq. (8), where  $x_f$  represents the ammonia mass fraction in fluid phase,  $x_g$  represents the ammonia mass fraction in the vapor phase and  $ex_{Ch,H_2O_v}^0$  represents the standard chemical exergy of vapor water.

$$ex_{Ch,NH_3,H_2O_L} = (1-q) \cdot [x_f \cdot ex_{Ch,NH_3}^0 + (1-x_f) \cdot ex_{Ch,H_2O_L}^0] \quad (6)$$

$$ex_{Ch,NH_3,H_2O_v} = q \cdot [x_v \cdot ex_{Ch,NH_3}^0 + (1-x_v) \cdot ex_{Ch,H_2O_v}^0] \quad (7)$$

$$ex_{Ch} = ex_{Ch,NH_3,H_2O_L} + ex_{Ch,NH_3,H_2O_v} \quad (8)$$

At last if the quality of the flow is 1 or higher, the chemical exergy is evaluated using Eq. (9). We extracted from Kotas (1985) the standard chemical exergy of the components. The value for liquid water standard chemical exergy,  $ex_{Ch,H_2O_L}^0$ , is 3120 kJ/kmol, for vapor water standard chemical exergy,  $ex_{Ch,H_2O_v}^0$ , the value is 11720 kJ/kmol and the ammonia standard chemical exergy,  $ex_{Ch,NH_3}^0$ , 341250 kJ/kmol.

$$ex_{Ch} = x \cdot ex_{Ch,NH_3}^0 + (1-x) \cdot ex_{Ch,H_2O_v}^0 \quad (9)$$

The definition of Fuel and Product, presented in table 2, guides the elaboration of the productive diagram of the cycle, presented in Fig. (3). Such diagram complements the thermal scheme (Fig. 1) and set the formation of the exergetic cost through the process. The productive diagram construction was based in a modification of the Structural Theory of the Exergetic Cost, in which the dissipations flows is partitioned in the units according to their entropy generation. Two dissipative units are present in the analyzed cycle, the condenser 1 and condenser 2, it was assumed that the exergy dissipated by the condenser 1 is allocated only in the boiler, separator 1, superheater, turbine 1 and condenser 1, while the exergy dissipated by the condenser 2 is allocated in the remainder equipment. The continuous lines in the diagram represent total flow of exergy, the red dashed lines represent exergy ratio of the condenser 1 and blue dashed lines represent the ratio of condenser 2, then they are divided in bifurcation 5 and 11 respectively. The dashed lines are fictitious flows, they are an assumption to equalize and internalize the dissipated exergy. For the development of the productive diagram, it is assumed that a real exergy flow cannot have two distinct natures, except when the ratio of the dissipation is incorporated to the fuels of the cycle components. This way, it is not plausible to combine mechanical work with thermochemical exergy.

Table 2. Productive structure for the Kalina cycle.

Unit	$\dot{F}$	$\dot{P}$
Boiler <sup>1</sup>	$E_{27}-E_{26}+\rho_{BO} \cdot (E_{32}-E_{31})$	$E_7-E_6$
Separator 1	$E_7+\rho_{S1} \cdot (E_{32}-E_{31})$	$E_8+E_{14}$
Separator 2	$E_{10}+\rho_{S2} \cdot (E_{30}-E_{29})$	$E_{11}+E_{17}$
Superheater	$E_{28}-E_{27}+\rho_{SU} \cdot (E_{32}-E_{31})$	$E_9-E_8$
Turbine 1	$E_{10}-E_9+\rho_{T1} \cdot (E_{32}-E_{31})$	$W_{LT1}+W_{P1}$
Turbine 2	$E_{11}-E_{12}+\rho_{T2} \cdot (E_{30}-E_{29})$	$W_{LT2}+W_{P2}$
Valve 1	$E_{15}+\rho_{V1} \cdot (E_{30}-E_{29})$	$E_{16}$
Valve 2	$E_{18}+\rho_{V2} \cdot (E_{30}-E_{29})$	$E_{19}$
Valve 3	$E_{25}+\rho_{V3} \cdot (E_{30}-E_{29})$	$E_1$
Absorber 1	$E_{25}+E_{16}+\rho_{A1} \cdot (E_{30}-E_{29})$	$E_{24}$
Absorber 2	$E_{12}+E_{19}+\rho_{A2} \cdot (E_{30}-E_{29})$	$E_{13}$
Pump 1	$W_{P1}+\rho_{P1} \cdot (E_{30}-E_{29})$	$E_3-E_2$
Pump 2	$W_{P2}+\rho_{P2} \cdot (E_{30}-E_{29})$	$E_{22}-E_{21}$
Regenerator 1	$E_{14}-E_{15}+\rho_{R1} \cdot (E_{30}-E_{29})$	$E_6-E_5$
Regenerator 2	$E_{17}-E_{18}+\rho_{R2} \cdot (E_{30}-E_{29})$	$E_5-E_4$
Regenerator 3	$E_{24}-E_{25}+\rho_{R3} \cdot (E_{30}-E_{29})$	$E_4-E_3$
Regenerator 4	$E_{13}-E_{20}+\rho_{R4} \cdot (E_{30}-E_{29})$	$E_{23}-E_{22}$
Condenser 1	$E_1-E_2+\rho_{C1} \cdot (E_{32}-E_{31})$	$E_{32}-E_{31}$
Condenser 2	$E_{20}-E_{21}+\rho_{C2} \cdot (E_{30}-E_{29})$	$E_{30}-E_{29}$

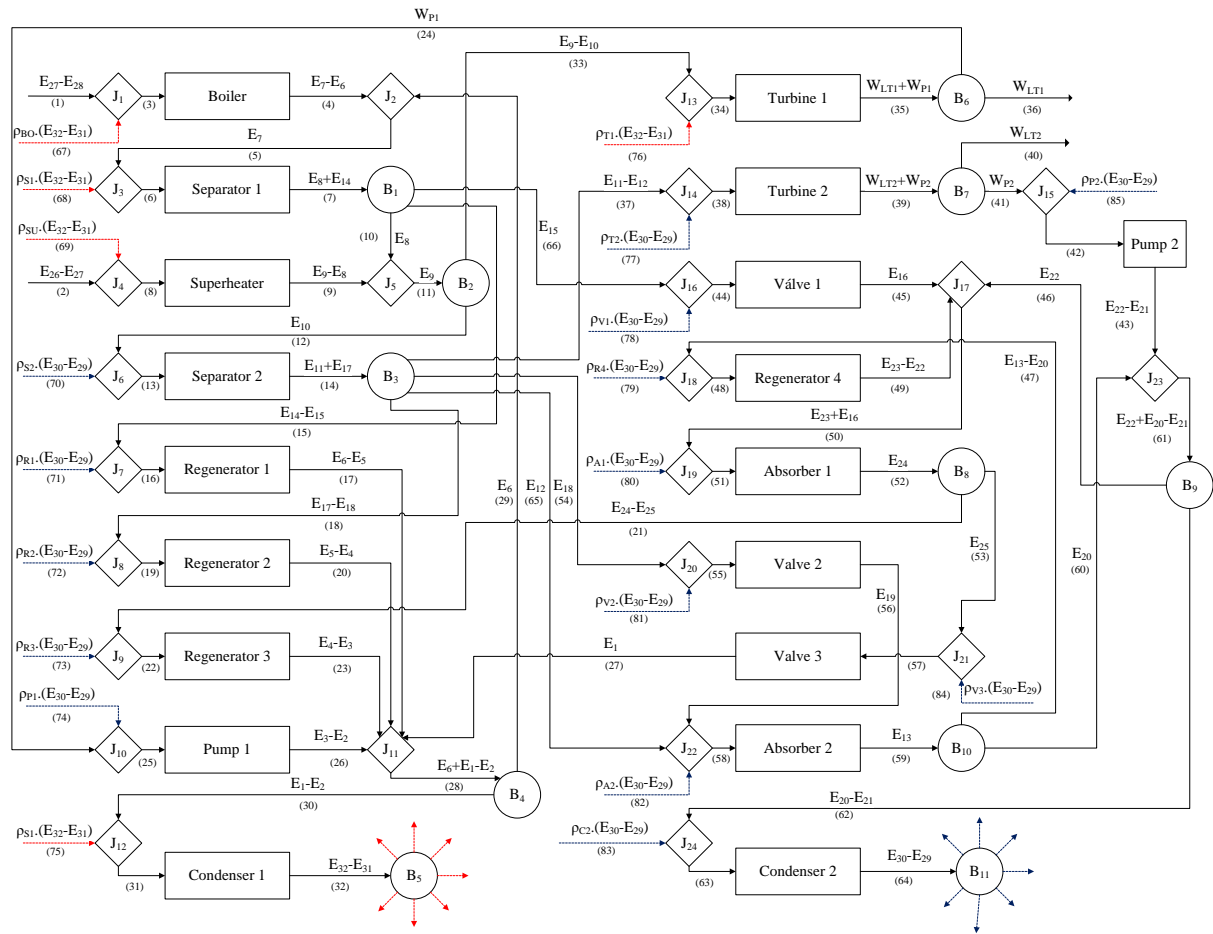


Figure 3. Representation of the productive diagram.

The thermoeconomic parameters for the 85 flows in the productive diagram were solved by EES. The resolution and optimization has as the main objective to find the minimum exergetic cost for each flow, specially the flows 36 and 40 which represent the net exergy output from turbine 1 and turbine 2. One equation is defined for each component of the productive diagram, forming 19 equations, as shown in Eq. (10). It establishes that the unit exergetic cost for each input flow is 1, then 2 equations are formed, Eq. (11). Each junction generate one equation of thermoeconomic balance, Eq (12), causing 24 equations are generated. Each bifurcation forms as many equations as exits therefore 40 equations are defined. The total of equations is 85, as many flows are present in productive diagram, Eq. (13). For the equation below,  $k^*$  represents the unit exergetic cost,  $B^*$  is the total exergetic cost, and it is evaluated by Eq. (14).

$$\dot{E}x_{out}k_{out}^* - \dot{E}x_{in}k_{in}^* = 0 \quad (10)$$

$$k_{input}^* = 1 \quad (11)$$

$$\dot{E}x_{out}k_{out}^* - \sum \dot{E}x_{in}k_{in}^* = 0 \quad (12)$$

$$k_{out}^* - k_{in}^* = 0 \quad (13)$$

$$k_j^* = \frac{B_j^*}{Ex_j} \quad (14)$$

The evaluation, predictions of the equipment and units cost, for exergoeconomic were based the cost information curves from National Energy Technology Centre (USA) with values corrected to the end of 2013. The information of the cost indexes is present in Tab. 3. For economic analysis the model included the whole cycle as a single equipment and the information of electricity cost is different for the turbine 1 and turbine 2. It is assumed that the preheater gases have zero cost, because they are a waste of cement production and usually are discharged in the environment.

Table 3. Cost Indexes.

Index	Value
Specific investment cost	973000 US\$/MW
Reference plant capacity	6.00 MW
O&M Cost	96 US\$/MWh
2013 Cost index	100
1958 Cost index	175
Yearly Operation Hours	6000 h
Interest rate	5%
Expected service life	20 years
Exchange rate (31/12/2013)	2.34 R\$/US\$

### 3. RESULTS AND DISCUSSION

The Cycle was optimized using genetic algorithm provided by the software EES as the optimization aimed to produce the maximum net power. The exergetic analysis of the results are shown in table 4. The equipment which generates the highest irreversibility rate are the turbines 1, 2, and the evaporator, although their exergy efficiencies are not the lowest. The highest exergetic cost occurs in Regenerators 1, 2 and 3, but since the Fuel amounts aren't high their inefficiencies don't effect on the overall performance factors. In this optimization, the proposed Kalina cycle was able to generate 1748 kW with the exergetic efficiency of 45.5%. The optimized parameters of the cycle are the ammonia mass fraction of 0.80, the first turbine inlet pressure of 140 bar and the second turbine inlet pressure of 27 bar.

Table 4. Optimized exergetic results.

Equipment	$\eta_{ex,i}$	$F_i$	$P_i$	$I_i$	k
Evaporator	0.793	2984.361	2366.315	618.046	1.261
Separator 1	1.000	91892.954	91892.813	0.141	1.000
Superheater	0.968	859.692	832.154	27.538	1.033
Turbine 1	0.983	82857.367	81462.099	1395.268	1.017
Separator 2	1.000	81462.099	81462.099	0.000	1.000
Turbine 2	0.990	81289.515	80501.125	788.391	1.010
Regenerator 1	0.484	44.261	21.401	22.860	2.068
Regenerator 2	0.608	0.377	0.229	0.148	1.646
Regenerator 3	0.631	226.406	142.923	83.483	1.584
Regenerator 4	0.883	885.562	782.026	103.536	1.132
Absorber 1	1.000	90218.849	90217.112	1.738	1.000
Absorber 2	1.000	80673.276	80673.158	0.118	1.000
Válve 1	0.995	9823.338	9772.427	50.911	1.005
Válve 2	1.000	172.207	172.151	0.056	1.000
Válve 3	0.998	89990.706	89789.489	201.216	1.002
Pump 1	1.000	89379.246	89362.086	17.159	1.000
Pump 2	1.000	79664.970	79664.397	0.574	1.000
Condenser 1	0.759	537.230	407.977	129.253	1.317
Condenser 2	0.904	126.833	114.601	12.231	1.107

The results of the thermoeconomic flows are shown in Tab. 5, the flows 36 and 40 represents the net power output. In the optimization the units exergetic cost of the electricity produced by the turbine 1 was 2.23 kW/kW and for the turbine 2 was 2.14 kW/kW. The total cost of the electricity was 213 R\$/MWh. The net power produced by the first turbine was 1116 kW and the second turbine was 633 kW, with the total power of 1749 kW. The results of the ratio of dissipated exergy is not presented in Tab. 5. This dissipation is represented by the flow 32 and 64 with the unit exergetic cost of 2.22 kW/kW for the condenser 1 and 1.76 kW/kW for the condenser 2.

Table 5. Optimized thermoeconomic results for selected flows.

Flow	Bi	$K_i^*$	$B_i^*$	Flow	Bi	$K_i^*$	$B_i^*$	Flow	Bi	$K_i^*$	$B_i^*$
1	2984.36	1.00	2984.00	23	142.92	2.59	369.70	45	9772.43	1.59	15498.00
2	859.69	1.00	859.70	24	126.99	2.23	283.50	46	79664.40	1.57	125198.00
3	3100.55	1.05	3242.00	25	128.52	2.23	286.10	47	885.56	1.57	1392.00
4	2366.31	1.37	3242.00	26	109.83	2.61	286.10	48	894.81	1.57	1408.00
5	91892.95	1.58	144900.00	27	89789.49	1.58	141779.00	49	782.03	1.80	1408.00
6	91892.98	1.58	144900.00	28	90063.87	1.58	142509.00	50	90218.85	1.58	142104.00
7	91892.81	1.58	144900.00	29	89526.64	1.58	141659.00	51	90327.71	1.57	142104.00
8	864.87	1.01	871.20	30	537.23	1.58	850.10	52	90217.11	1.58	142104.00
9	832.15	1.05	871.20	31	561.53	1.61	903.90	53	89990.71	1.58	141747.00
10	82025.21	1.58	129341.00	32	407.98	2.22	903.90	54	172.21	1.57	270.60
11	82857.37	1.57	130212.00	33	1395.27	1.57	2193.00	55	172.21	1.57	270.60
12	81462.10	1.57	128019.00	34	1657.56	1.67	2774.00	56	172.15	1.57	270.60
13	81462.10	1.57	128019.00	35	1242.66	2.23	2774.00	57	90008.69	1.58	141779.00
14	81462,1	1,57	128019	36	1115.67	2.23	2490.00	58	344.37	368.20	126780.00
15	44.26	1.58	69.79	37	788.39	1.57	1239.00	59	80673.16	1.57	126780.00
16	46.30	1.59	73.38	38	858.84	1.59	1363.00	60	79787.60	1.57	125388.00
17	21.40	3.43	73.38	39	637.24	2.14	1363.00	61	79791.23	1.57	125397.00
18	0.38	1.57	0.59	40	633.04	2.14	1354.00	62	126.83	1.57	199.30
19	0.39	1.58	0.62	41	4.21	2.14	9.00	63	127.93	1.57	201.20
20	0.23	2.69	0.62	42	4.26	2.13	9.09	64	114.60	1.76	201.20
21	226.41	1.58	356.60	43	3,63	2,5	9,09	65	80501.12	1.57	126509.00
22	233.87	1.58	369.70	44	9827.89	1.58	15498.00	66	9823.34	1.58	15490.00

Analyzing the variation of ammonia mass fraction in the boiler outlet, the graphs in Fig. (4) and Fig. (5) show that the increasing in the ammonia mass fraction rise the total power output and the cost of the electricity, except when the quality is 0.85. In this scenario, the maximum power is obtained with 0.78 of ammonia mass fraction and then starts to decrease with values higher than the aforementioned. The increase of the quality also increases the power output and the costs as well. It is verified that the power produced in the second turbine decreases with the increase of ammonia mass fraction, but the gain in power produced in the first turbine is higher than the decrease observed in the second one. The maximum power obtained with quality of 0.9 and 0.85 was 1752 kW and 1708 kW respectively. The maximum power of the turbine 1 was 825.3 kW, 817.2 kW and 807.2 kW for the quality of 0.95, 0.90 and 0.85 respectively, the same results for turbine 2 was 1001.8 kW, 975.0 kW and 947.7 kW, respectively. The exergetic cost  $k_{40}^*$ , correlated to the second turbine has a slight change with ammonia mass fraction, while  $k_{36}^*$ , correlated with the first turbine has a considerable change. The parameter  $k_{40}^*$  varies from 2.014 kW/kW to 1.957 kW/kW with the quality of 0.95, and from 2.009 kW/kW to 1.971 kW/kW with the quality of 0.9 and from 2.011 kW/kW to 1.984 kW/kW with the quality of 0.85. The parameter  $k_{36}^*$  ranges from 2.405 kW/kW to 2.392 kW/kW with the quality of 0.95, with the quality of 0.9 it ranges from 2.499 kW/kW to 2.463 kW/kW and with the quality of 0.85 it ranges from 2.399 kW/kW to 2.347 kW/kW. In this analysis, the  $\Delta T$  of the superheater is set at 15K and the pressure of the boiler is set at the 140 bar.

The variation of the superheater temperature difference, between the states 9 and 26, is shown in Fig. (6) and Fig. (7). It is verified that as the increase of this temperature rises, the power output also is increased to a certain level, then it starts to decrease. It is also verified that this temperature difference has a large influence in the power output of the turbines 1 and 2. While the power produced in turbine 2 is always increasing with the temperature difference, the opposite behavior occurs in in turbine 1. The behavior of the quality tends to behave the same as the first analysis, the increase of this variable represents gain of power and cost addition. The unit exergetic cost of the power of turbine 2 is again slightly increased and the unit exergetic cost of turbine 1 slightly decreases.

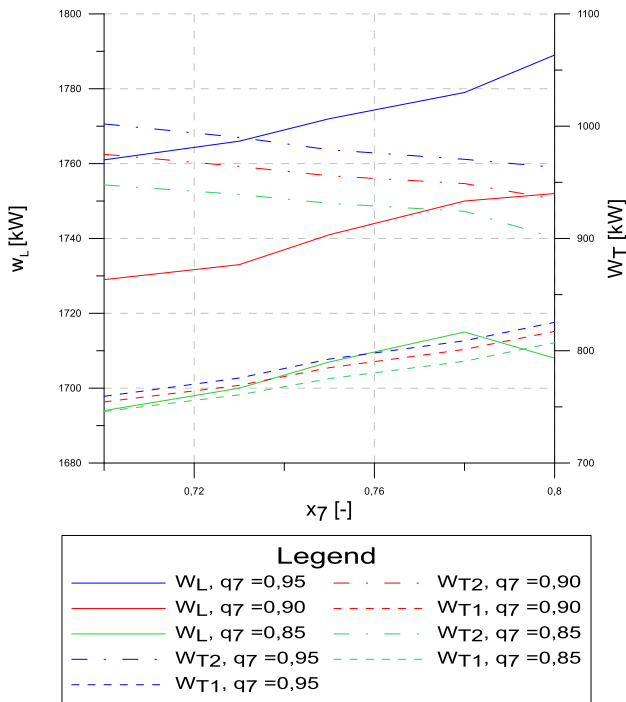


Figure 4. Power output of the cycle in function of ammonia mas fraction

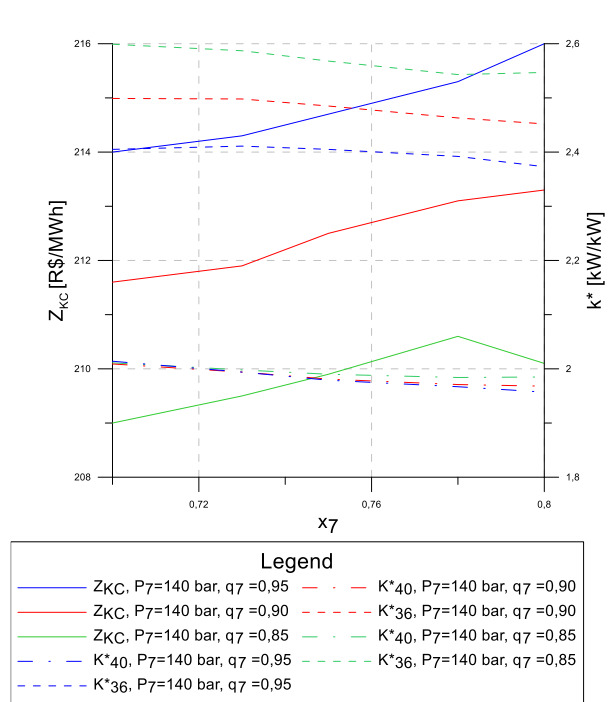


Figure 5. Cost and unit exergetic cost in function of ammonia mass fraction

In this analysis the unit exergetic cost  $k^*_{40}$ , ranges from 1.952 kW/kW to 1.984 kW/kW and the unit exergetic cost  $k^*_{36}$ , ranges from 2.383 kW/kW to 2.371 kW/kW with the quality of 0.95. The results with quality of 0.9 varies from 2.009 kW/kW to 1.971 kW/kW for  $k^*_{40}$  and 2.463 kW/kW to 2437 kW/kW for  $k^*_{36}$ . At last, for the quality of 0.85,  $k^*_{40}$  and  $k^*_{36}$  ranges from 1.996 kW/kW to 2.029 kW/kW and from 2.332 kW/kW to 2.529 kW/kW. Analyzing the superheater temperature difference, the highest electricity generation cost is 215 R\$/MWh, producing 1780 kW and in the lowest generation, the values are 209 R\$/MWh and 1693 kW, respectively.

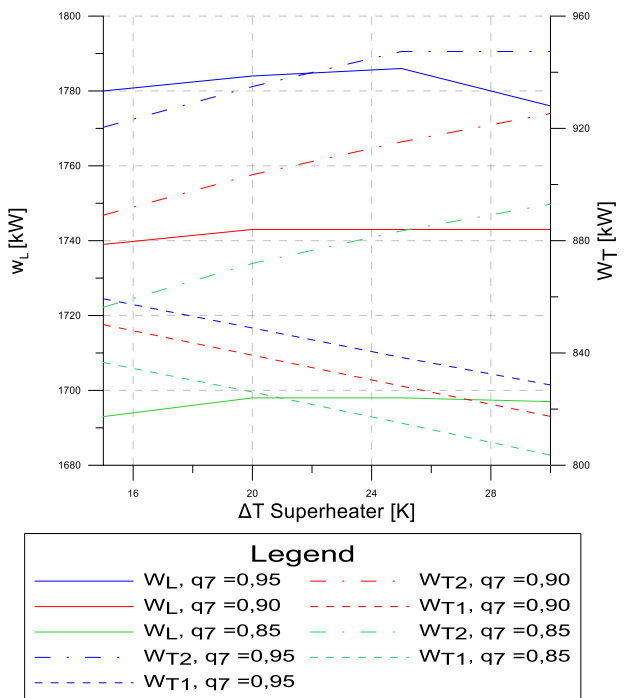


Figure 6. Power output of the cycle in function of temperature difference in superheater

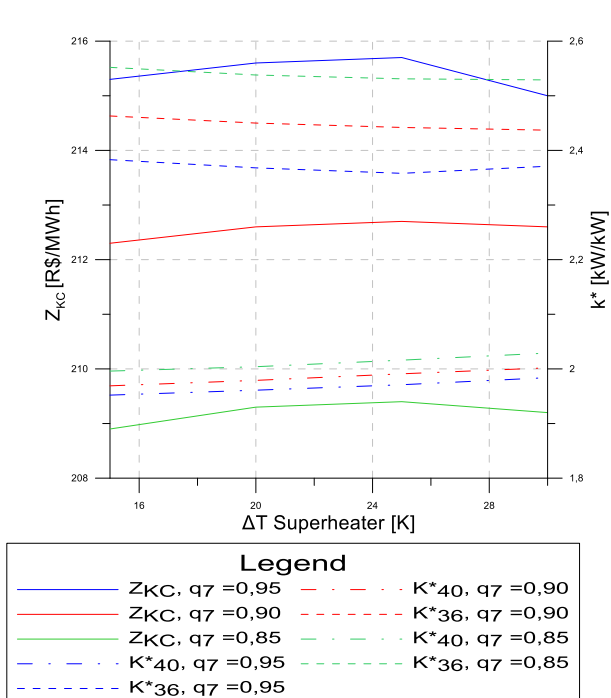


Figure 7. Cost and unit exergetic cost in function of temperature difference in superheater

#### 4. CONCLUSIONS

From the thermoeconomic analysis, based on EES (Engineering Equation Solver) model, of a Kalina cycle for waste heat recovery we concluded that:

- The generated power is directly linked to the generation cost for the same parameters. Therefore the greater the power, the higher the cost of generation is;
- The quality of the steam leaving the evaporator is also directly linked to the power generated, so is the generation cost, increasing the cost from 209 R\$/MWh to 215 R\$/MWh. This is a parameter that must be observed to predict the feasibility of the economic cycle deployment;
- The exergetic unit cost of the turbine 1 is more sensitive than the exergetic unit cost of the turbine 2 to the evaluated parameters, but it is interesting to evaluate what parameters have direct influence on the cost of turbine 2;
- The maximization of the power generates 1780 kW with the cost of 215 R\$/MWh and is compatible with the market prices at the end of 2013;
- The lowest cost of generation is 209 R\$/MWh and it is found when the cycle produces 1693 kW of power and still is compatible with the market prices at the end of 2013.

#### 5. ACKNOWLEDGEMENTS

The authors thank FAPEMIG, FAPEMIG/CEMIG APQ-03422-12 research project, ANNEL Research and Developed program (P&D) research project GT0554 and Pontifical Catholic University of Minas Gerais – PUC Minas for the financial support to this work.

#### 6. REFERENCES

- Arrieta, F.T.P., and Horta, G.R.C., 2014. “Análise Exergética e Termoeconômica de Ciclo Kalina Simples Suprido Por Fontes De Baixa Temperatura.”. In Proceedings of the XXXV Ibero-Latin American Congress on Computational Methods in Engineering, Fortaleza, Ceará, Brasil.
- Arrieta, F.T.P. and Santos, L.A.O., 2014. “Modelagem Termodinâmica e Exergética de um Ciclo Kalina Para a Cogeração na Indústria de Cimento”. In Proceedings of the ABCM 2014 VIII Congresso Nacional de Engenharia Mecânica, Uberlândia, Minas Gerais, Brasil.
- Arslan, O., 2011, “Power generation from medium temperature geothermal resources: ANNbased optimization of Kalina cycle system-34”, *Energy*, Vol. 36, pp. 2528-2534.
- Cimento Apodi (Ceará), 2015, “WHRS - UTE CIMENTO APODI WASTE HEAT RECOVERY SYSTEM: Sistema De Recuperação De Calor”. Quixeré, 15 slides: color.
- Elsayed, A., Mebrahtu, E., Al-Dadah, R., Mahmoud, S, and Rezk, Ahmed; 2013 “Thermodynamic performance of Kalina cycle system 11 (KCS11): feasibility of using alternative zeotropic mixtures”. *International Journal of Low-Carbon Technologies*, Vol. 8, i69-i78.
- He, J., Liu, C., Xu, X., Li, Y., Wu, S., and Xu, J.; 2014. “Performance research on modified KCS (Kalina cycle system) 11 without throttle valve”, *Energy*, Vol. 64, p 389-397.
- Junior, E.P.B., Arrieta, F.T.P, Irokawa, G.N.F. and Santos, L.A.O., 2014. “Avaliação Termoeconômica de um Ciclo Kalina Para a Recuperação De Calor Residual”. In Proceedings of the XXXVI Ibero-Latin American Congress on Computational Methods in Engineering, Rio de Janeiro, Rio de Janeiro, Brasil.
- Kotas, T.J, 1985. *The Exergy Method of Thermal Plant Analysis*. Butterworths, London.
- Mirolli, M. D., 2005, “The Kalina Cycle for Cement Kiln Waste Heat Recovery Power Plants”, *IEEE*, p. 330-336.
- Lolos, P.A., and Rogdakis, E.D., 2009, “A Kalina power cycle driven by renewable energy sources”, *Energy* Vol. 34, pp. 457-464.
- Rodriguez, C.E.C., Palacio, J.C.E., Venturini, O.J., Lora, E.E.S., Cobas, V.M., Santos, D.M., Dotto, F.R.L., and GIALLUCA, V.; 2013, “Exergetic and economic comparison of ORC and Kalina cycle for low temperature enhanced geothermal system in Brazil”. *Applied Thermal Engineering*, Vol. 52, p 109-119.
- Singh, O. K., and Kaushik, S.C.; 2013 “Energy and exergy analysis and optimization of Kalina cycle coupled with a coal fired steam power plant”. *Applied Thermal Engineering*, Vol. 51, p 787-800, 2013.

#### 7. RESPONSIBILITY NOTICE

The authors are the only responsible for the printed material included in this paper.